Electronic Supplementary Material (ESI) for Physical Chemistry Chemical Physics.

Supporting Information

Enhancing the photoluminescence of surface anchored metal-organic frameworks: mixed linkers and efficient acceptors

M. Oldenburg[a], A. Turshatov[a], D. Busko[a], M. Jakoby[a], R. Haldar[b], K. Chen[c], G. Emandi[d], M. O. Senge[d], C. Wöll[b], J.M. Hodgkiss[c], B. S. Richards[a,e], I. A. Howard[a,e,*]

[a]*Institute of Microstructure Technology, Karlsruhe Institute of Technology, Hermann-von-Helmholtz-Platz 1, 76344 Eggenstein-Leopoldshafen, Germany*
[b]*Institute of Functional Interfaces, Karlsruhe Institute of Technology, Hermann-von-Helmholtz-Platz 1, 76344 Eggenstein-Leopoldshafen, Germany*
[c]*The MacDiarmid Institute for Advanced Materials and Nanotechnology, and School of Chemical and Physical Sciences, Victoria University of Wellington, Wellington 6140, New Zealand*
[d]*School of Chemistry, SFI Tetrapyrrole Laboratory, Trinity Biomedical Science Institute, 152-160 Pearse Street, Trinity College Dublin, The University of Dublin, Dublin 2, Ireland*
[e]*Light Technology Institute, Karlsruhe Institute of Technology, Engesserstrasse 13, 76131 Karlsruhe, Germany*

S I. Structure of ADB SURMOF by X-Ray diffractometry

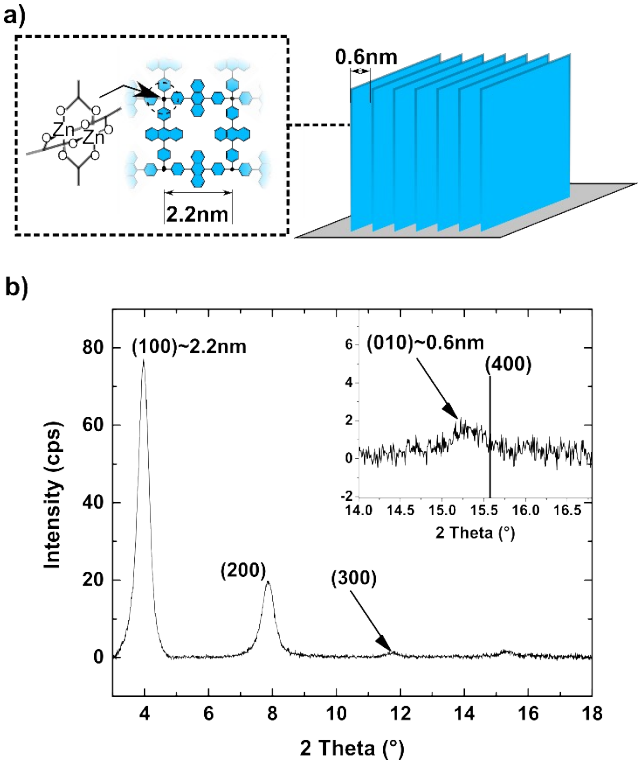

Figure S 1: a) Schematic of the ADB SURMOF. The intra-layer distance of 2.2 nm corresponds to the miller indices (100). The distance of 0.6 nm corresponds to the miller index (010). b) In-plane XRD for an ADB SURMOF on silicon showing three orders of (100) peak. Inset: Zoom into the region where the first order of the (010) peak appears together with the predicted position of the fourth order of (100).

S II. Photoluminescence quantum yield, LUMOGEN Violet in PMMA as a standard

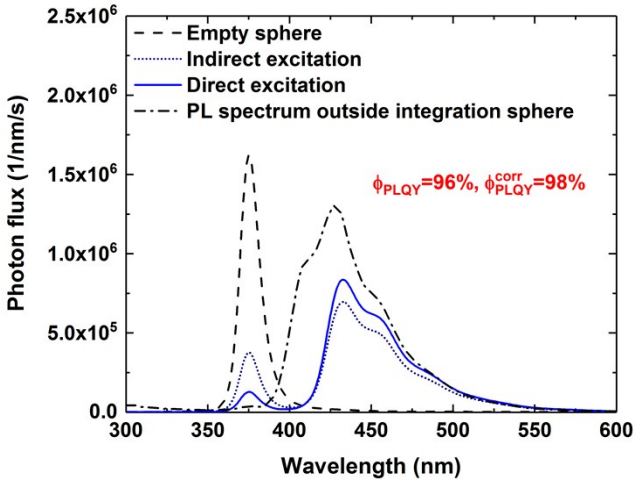

Figure S 2: Shown are the recorded spectra of the photoluminescence quantum yield (PLQY) measurement of a PMMA slide with LUMOGEN violet dye. For reabsorption correction, the spectrum outside the sphere was recorded.[1] For correction the ratio a was used between the area of the spectrum that was recorded outside the integration sphere, and the area of the spectrum that was directly excited in the integration sphere. The following equation was used for reabsorption correction: $$\phi_{PLQY}^{corr} = \frac{\phi_{PLQY}}{(1 - a + a\phi_{PLQY})}.$$

S III. Overlap of ADB emission spectrum and coumarin 343 and coumarin 334 absorption spectrum

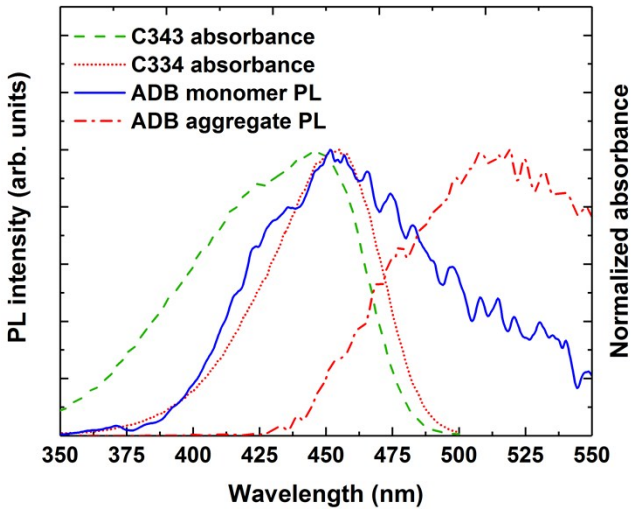

Figure S 3: The emission spectrum of ADB the monomer and aggregate state are shown together with the absorbance spectra of coumarin 343 (C343) and coumarin 334 (C334) solutions.

S IV. Bonding of Coumarin 343 within the ADB SURMOF

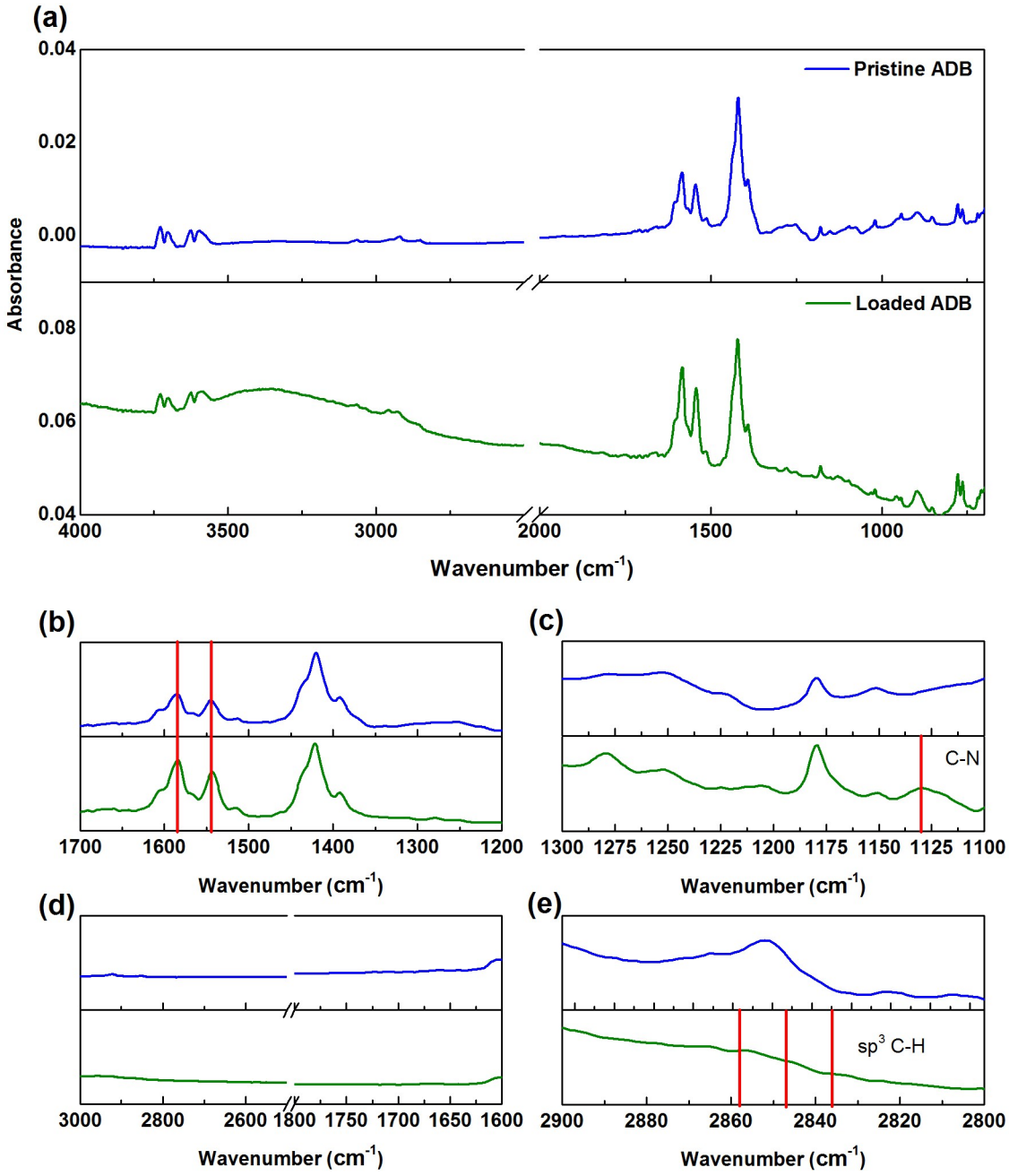

Figure S 4: a) Infrared reflection-absorption spectrum (IRRAS) of an ADB SURMOF grown on MHDA/Au substrate (upper panel, blue line) and ADB SURMOF loaded with coumarin 343 (lower panel, green line). The broad band around 3400 cm^{-1} is the stretching of OH group coming from coumarin 343. This stretching is absent in the pristine ADB SURMOF. b) The bands at 1590 cm^{-1} and 1420 cm^{-1} are assigned to the asymmetric and symmetric stretching of COO^-, indicating the formation of a zinc paddle-wheel structure with bidentate ligands as the difference of both bands it between 140 and 200 cm^{-1}. [2] c) Shows the presence of a SURMOF band around 1130 cm^{-1} coming from coumarin 343, this band is absent in the pristine ADB spectrum. [3] d) Shows the absence of free carboxylic group vibrations in both, pristine ADB SURMOF and loaded ADB SURMOF. e) The absence of free carboxylic groups can be attributed to strong hydrogen bonds formation, which form sp^3 C-H bands around 2860, 2845 and 2835 cm^{-1} in the case of the loaded ADB SURMOF.

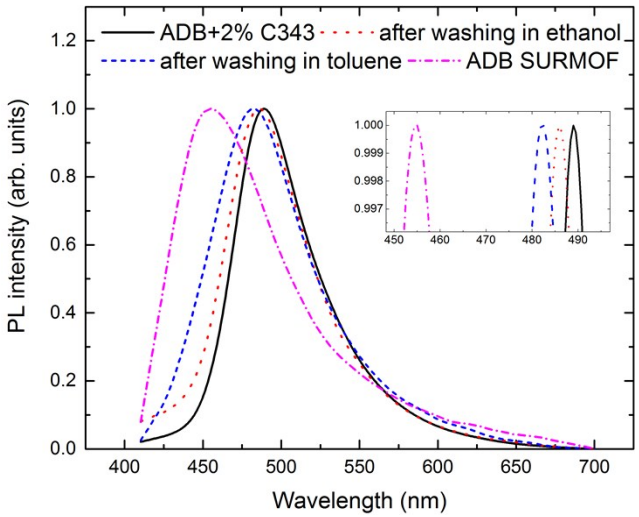

Figure S 5: Two ADB SURMOFs with 2% of coumarin 343 in the linker solution were synthesized and the emission spectrum was recorded (black). Both samples were then washed for 3 days in ethanol (red curve) and toluene solution (blue curve). As a comparison the spectrum of pristine ADB SURMOF (purple) is shown. The inset shows a magnification of the peak position of every curve.

S V. Difference between loading of coumarin 343 during SURMOF synthesis and loading via the drop-casting method

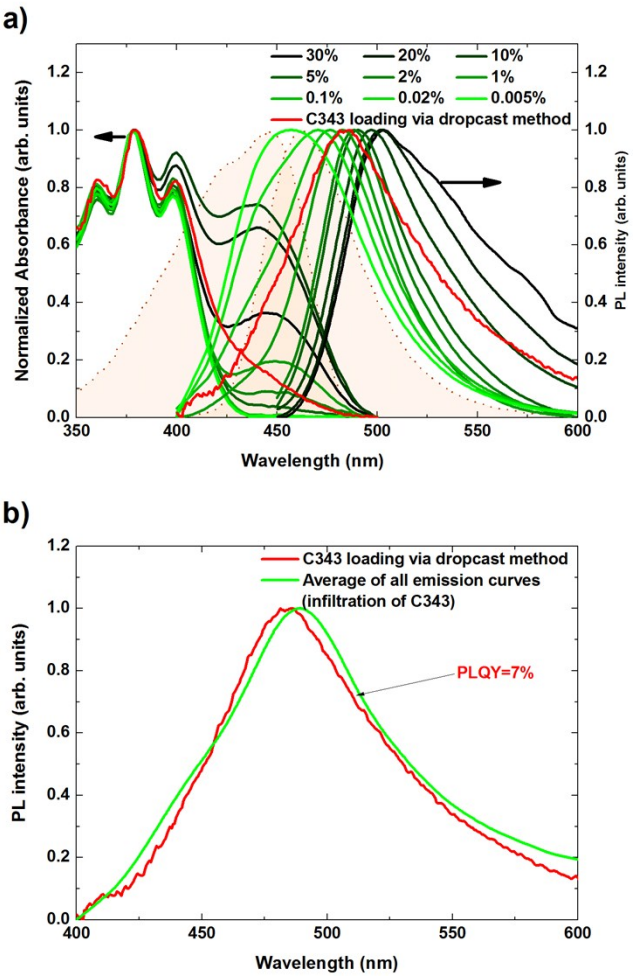

Figure S 6: This figure compares the different behavior in steady state PL between the loading of coumarin 343 (C343) which is described in the main text and loading of the ADB SURMOF post-synthesis via drop-casting of a 20 µM concentrated C343 solution on a pristine ADB SURMOF film. In the drop-casting technique, first the SURMOF is fabricated then the dye solution is drop-cast onto the SURMOF and allowed to dry. Finally the sample is rinsed with ethanol to remove the dye on the surface. Panel a) shows the normalized absorbance and PL emission spectrum of different ADB SURMOFs which were prepared with a defined molar ratio between ADB and C343 molecules (9 shades of green). Compared to this the absorbance and PL emission spectrum of an ADB SURMOF loaded with C343 are shown (red). The absorbance spectrum does not show a distinct peak at 450 nm. Further, the emission spectrum of the drop-casted sample shows a broad emission. Panel b) shows the emission spectrum of the drop-casted sample (red) and the average emission of all 9 samples which were loaded with C343 during the synthesis. The good overlap of both curves indicates that the drop-casting method leads to a non-uniform distribution of dyes in the ADB SURMOF leading to sectors with different concentrations of C343 loading within the ADB SURMOF.

S VI. Coumarin 334 within the ADB SURMOF and reproduction of the PLQY values

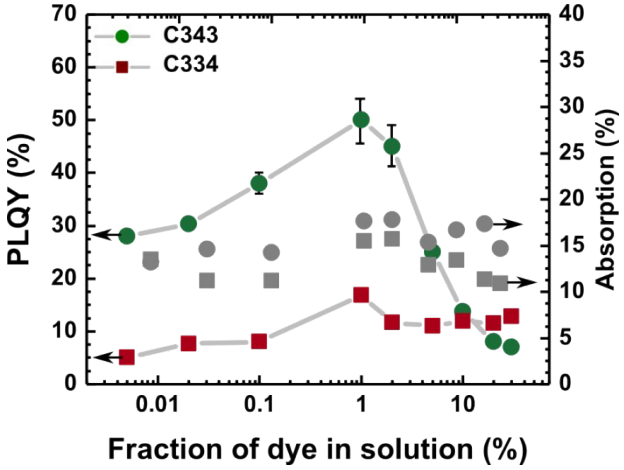

Figure S 7: The graph shows the PLQY and absorption measurement of ADB SURMOFs infiltrated by C343 and C334 as a function of the concentration of the dye in the ADB linker solution. Samples with 2%, 1% and 0.1% of C343 were repeated 3 times to estimate an error, which is indicated by the error bar.

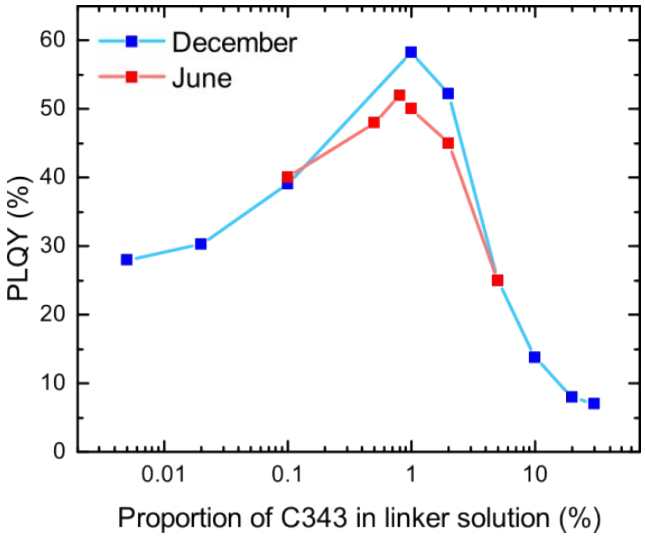

Figure S 8: The PLQY of ADB SURMOFs with varying proportions of coumarin 343 in the linker solution are shown for fabrication runs made in December and June in Karlsruhe, Germany. In both cases the trend is reproduced, with a clear peak in quantum yield around 1% loading. The slightly lower quantum yields obtained in summer may be due to the different ambient conditions in the preparation laboratory (humidity, temperature).

S VII. Estimation of the amount of C343 in ADB SURMOF via absorption measurement

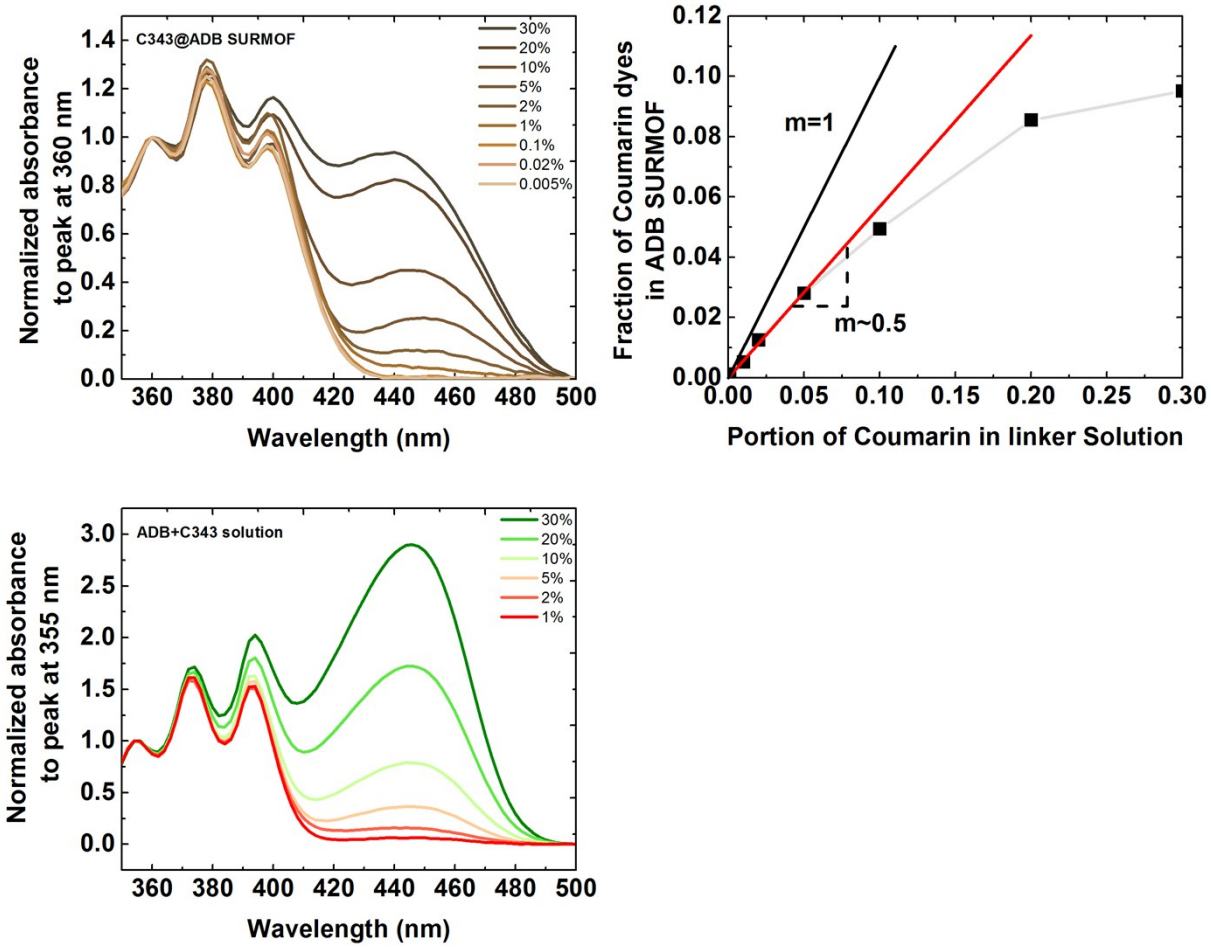

Figure S 9: (a) Top: Absorption spectra of ADB SURMOF with different C343 concentrations in the initial linker solution. Bottom: Absorption spectra of ADB solution with different C343 concentration. (b) Resulting correlation between the concentration of C343 in the SURMOF and the initial concentration. The red line indicates a linear dependence for low concentrations with a slope of roughly 0.5. As a reference, a linear function with the slope of 1 is plotted. The deviation at high concentrations indicates that C343 is interfering the proper formation of the ADB SURMOF.

S VIII. Singlet-singlet annihilation in ADB SURMOF

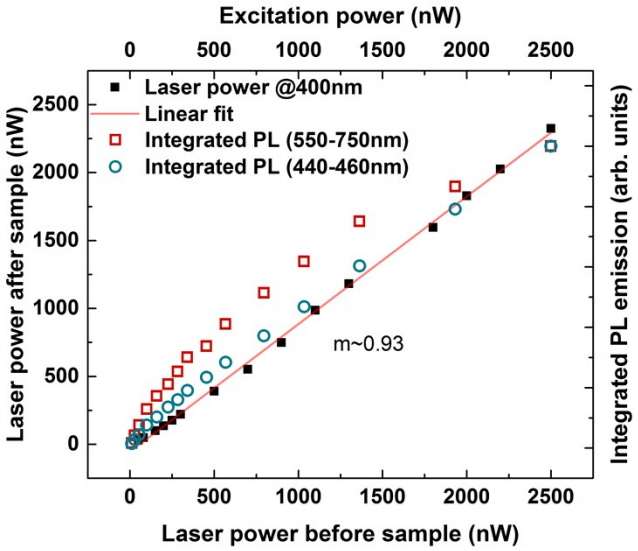

Figure S 10: Laser power measured before and after the sample for the intensity dependent measurement. The linear behavior shows that there is no absorption saturation effect.

Solving rate equations:

The rate equations of the form:

$$\frac{\partial A}{\partial t} = -kA - \gamma(t)A^2, A(0) = A_0$$

is a special case of the Bernoulli differential equation which can be transformed using:

$$\tilde{A} = \frac{1}{A}$$

into an easier linear differential equation:

$$\frac{\partial \tilde{A}}{\partial t} = k\tilde{A} - \gamma(t).$$

Three-dimensional case with time-independent γ:

$$\frac{\partial \tilde{A}}{\partial t} = k\tilde{A} - \gamma, \tilde{A}(0) = \tilde{A}_0 = \frac{1}{A_0}$$

$$\tilde{A} = \frac{\gamma(1 - \exp(-kt)) + k\tilde{A}_0 \exp(kt)}{k}$$

$$A = \frac{1}{\tilde{A}} = \frac{kA_0}{\exp(kt)(k + \gamma A_0) - \gamma A_0}.$$

This can be further integrated over time using the substitution $x = \exp(-kt)$:

$$\int_0^\infty A(t)dt = \int_0^\infty \frac{kA_0}{\exp(kt)(k+\gamma A_0) - \gamma A_0} dt$$
$$= \frac{k}{\gamma} \ln\left(1 + \frac{\gamma}{k} A_0\right).$$

One-dimensional case with time-dependent $\gamma(t) = 4\pi D R_0 \frac{R_0}{\sqrt{2\pi D t}} = \alpha/\sqrt{t}$

$$\frac{\partial \tilde{A}}{\partial t} = k\tilde{A} - \frac{\alpha}{\sqrt{t}}, \tilde{A}(0) = \tilde{A}_0$$

For large times this function should have the form $\tilde{A}(t) = \exp(kt)$, therefore we guess the following form for the general solution:

$$\tilde{A} = g(t)\exp(kt).$$

Inserting this into the equation above leads to a differential equation for $g(t)$:

$$g'(t) = -\frac{\alpha}{\sqrt{t}}\exp(kt)$$
$$g(t) = \int_0^t -\frac{\alpha}{\sqrt{t'}}\exp(kt')dt'$$

This can be integrated using the substitution $t' = -u^2$:

$$g(t) = 2\alpha \int_0^{-u^2} \exp(-ku^2)du$$
$$= \sqrt{\frac{\pi}{k}}\alpha \operatorname{erf}(-\sqrt{k}u^2) + c$$
$$= \sqrt{\frac{\pi}{k}}\alpha \operatorname{erf}(\sqrt{kt}) + c$$

so that:

$$\tilde{A} = \left(\sqrt{\frac{\pi}{k}}\alpha \operatorname{erf}(\sqrt{kt}) + c\right)\exp(kt),$$

where c is a constant, which can be found using the initial condition $\tilde{A}(0) = \tilde{A}_0$

$$\tilde{A} = \left(\sqrt{\frac{\pi}{k}}\alpha \operatorname{erf}(\sqrt{kt}) + \tilde{A}_0\right)\exp(kt).$$

Retransforming $\tilde{A}(t)$ back to $A(t)$ gives the final solution:

$$A(t) = \frac{1}{\tilde{A}} = \frac{A_0 \exp(-kt)}{A_0 \sqrt{\frac{\pi}{k}} \alpha \operatorname{erf}(\sqrt{kt}) + 1}.$$

Further integration did not lead to a known analytic expression.

S IX. SEM images of SURMOFs

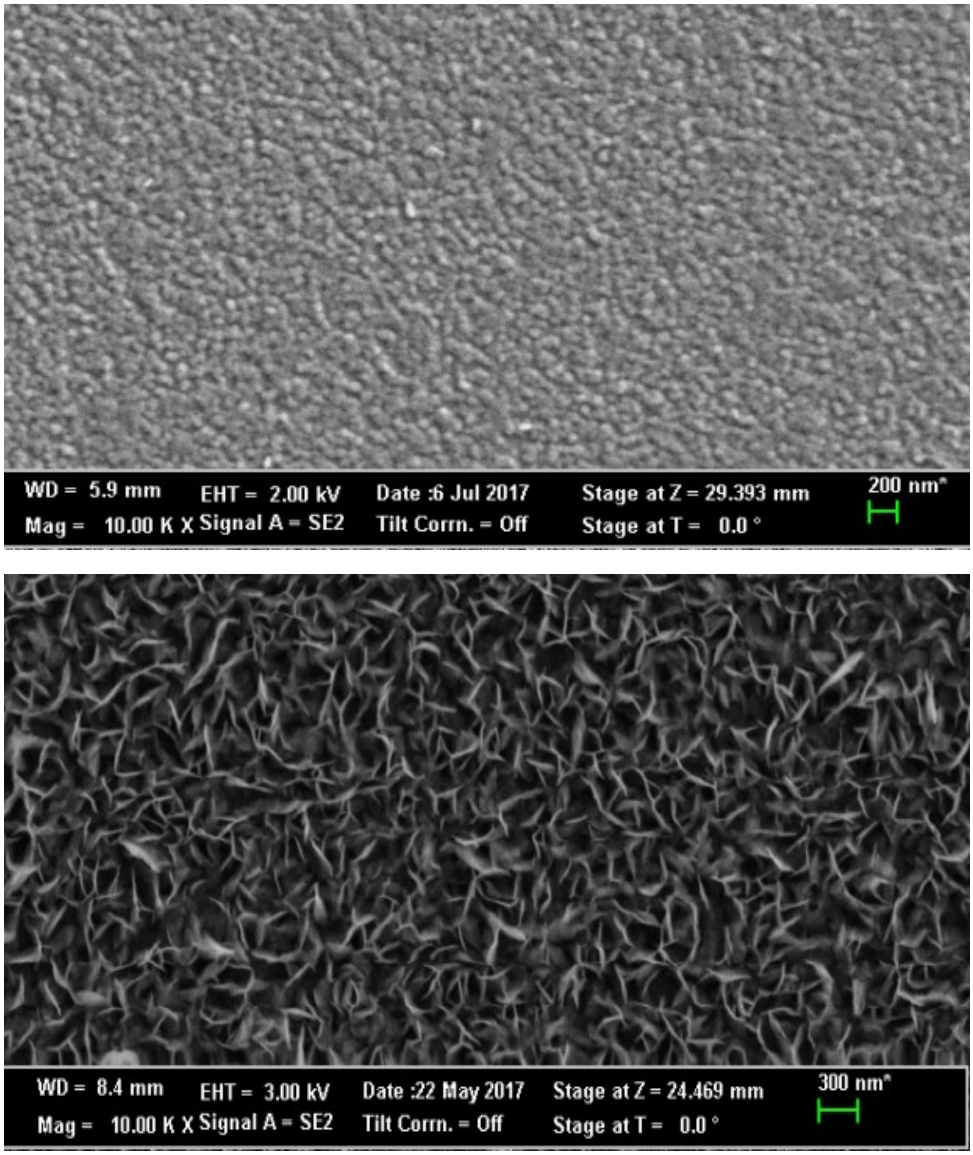

Figure S 11: SEM images (with a magnification of 10000) of the surface of ADB SURMOFs grown on soda lime glass substrate. Top: ADB SURMOF made by spin coating. Bottom: ADB SURMOF made by spray coating.

S X. Direct excitation of bilayers

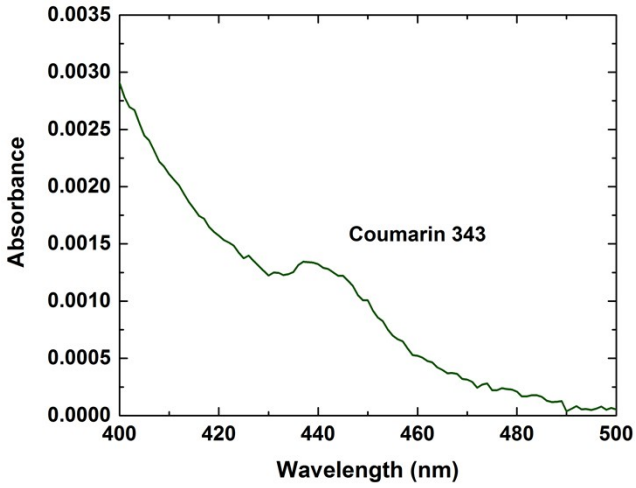

Figure S 12: Absorbance spectrum of C343@ADB spin coated SURMOF. The peak around 440 nm corresponds to the infiltrated coumarin 343 molecule.

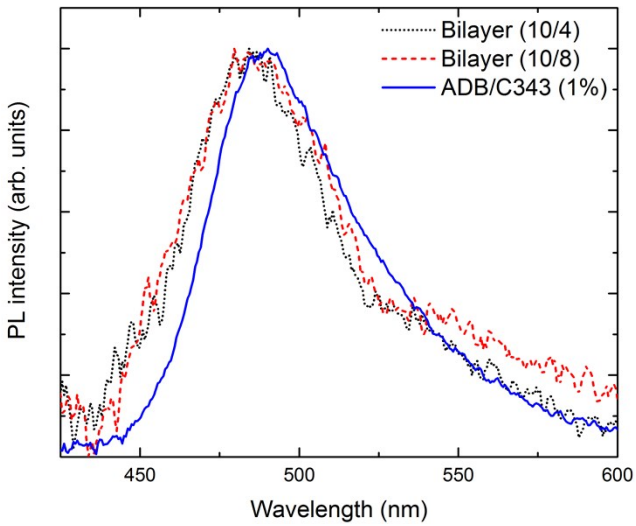

Figure S 13: PL spectra of ADB/C343 (1%) SURMOF and the bilayer SURMOFs made from a C343@ADB SURMOF (10 cycles) and Pd-DCP SURMOF (4 and 8 cycles) mentioned in the main text.

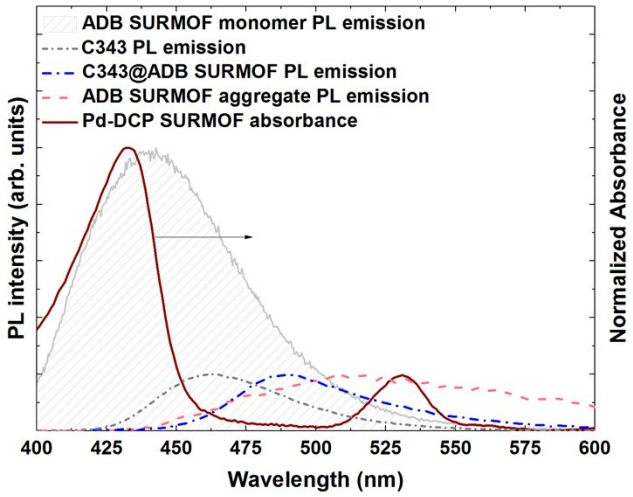

Figure S 14: Shown are the PL spectra for the ADB SURMOF monomer and aggregate emission, the C343 in ethanol solution and the ADB SURMOF loaded with C343. Further, the absorbance spectrum of Pd-DCP SURMOF is shown.

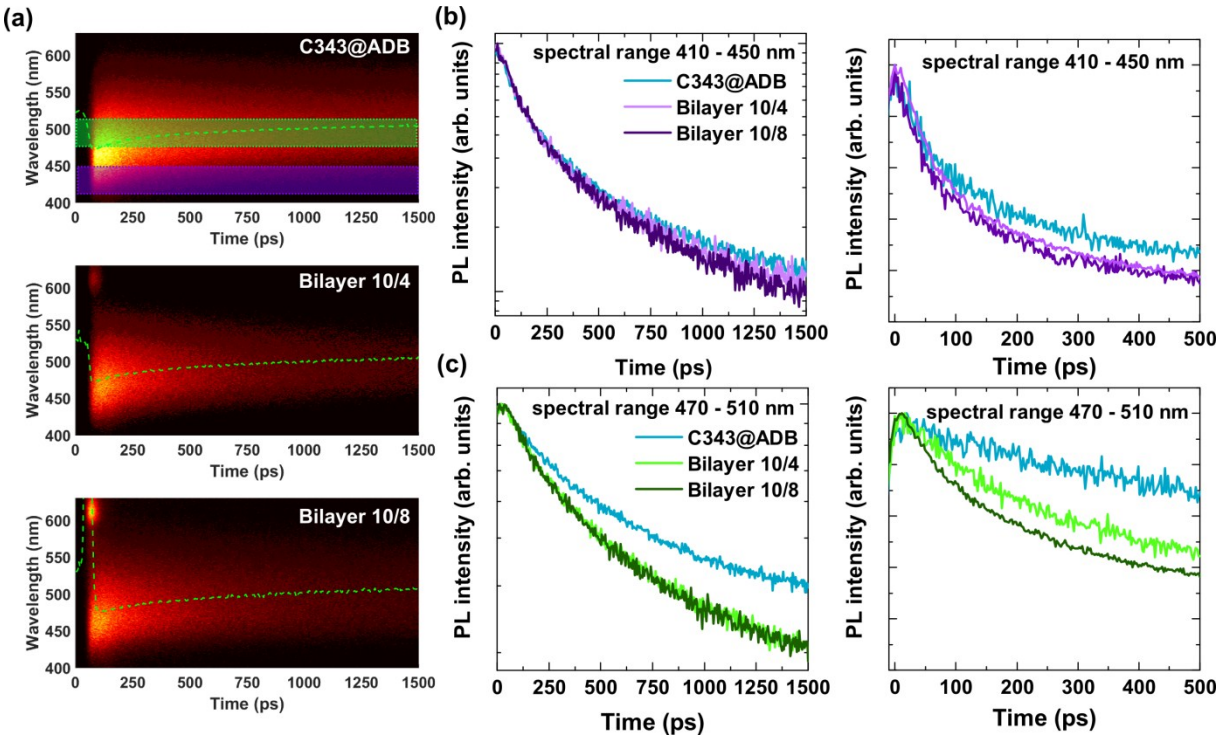

Figure S 15: (a) Streak camera measurements of the C343@ADB, bilayer 10/4 and bilayer 10/8. The green and violet areas indicate the spectral range, which were integrated over the wavelength to extract the corresponding transients. The green dashed line indicates the position of the maximum at a given time slice. (b) Transients for the spectral range 410 – 450 nm. Left: Time range 0 – 1500 ps. Right: Time range 0 – 500 ps. The transients show that the dynamic quenching in the bilayers via FRET back transfer is small. (c) Transients for the spectral range 470 – 410 nm. Left: Time range 0 – 1500 ps. Right: Time range 0 – 500 ps. The transients show that the dynamic quenching in the bilayers is significant for this spectral region.

1. Wilson, L. R.; Richards, B. S., *Appl. Opt.* **2009,** *48*, 212.
2. Tan, K.; Nijem, N.; Canepa, P.; Gong, Q.; Li, J.; Thonhauser, T.; Chabal, Y. J., *Chem. Mater.* **2012,** *24*, 3153.
3. Kanoo, P.; Haldar, R.; Cyriac, S. T.; Maji, T. K., *Chem. Commun.* **2011,** *47*, 11038.